SHABANA ANJUM

DOC-20260605-WA0002.

ANTENNA

Document Details

Submission ID

trn:oid:::27535:147973058

Submission Date

Aug 11, 2026, 6:15 PM GMT+5:30

Download Date

Aug 11, 2026, 6:16 PM GMT+5:30

File Name

DOC-20260605-WA0002..pdf

File Size

830.4 KB

21 Pages

4,535 Words

25,849 Characters

9% Overall Similarity

The combined total of all matches, including overlapping sources, for each database.

Filtered from the Report

- Small Matches (less than 10 words)

Match Groups

24 Not Cited or Quoted 7%
Matches with neither in-text citation nor quotation marks

5 Missing Quotations 2%
Matches that are still very similar to source material

0 Missing Citation 0%
Matches that have quotation marks, but no in-text citation

0 Cited and Quoted 0%
Matches with in-text citation present, but no quotation marks

Top Sources

3% Internet sources
5% Publications
4% Submitted works (Student Papers)

Integrity Flags

0 Integrity Flags for Review

Our system's algorithms look deeply at a document for any inconsistencies that would set it apart from a normal submission. If we notice something strange, we flag it for you to review.

A Flag is not necessarily an indicator of a problem. However, we'd recommend you focus your attention there for further review.

Match Groups

24 Not Cited or Quoted 7%
Matches with neither in-text citation nor quotation marks

5 Missing Quotations 2%
Matches that are still very similar to source material

0 Missing Citation 0%
Matches that have quotation marks, but no in-text citation

0 Cited and Quoted 0%
Matches with in-text citation present, but no quotation marks

Top Sources

3% Internet sources
5% Publications
4% Submitted works (Student Papers)

Top Sources

The sources with the highest number of matches within the submission. Overlapping sources will not be displayed.

1	Publication	Aneesha, Mohan Singh Mehata. "Reusable fluorescent WS2 QDs sensor for ultralo...	1%
2	Publication	Neha Bhatt, Mohan Singh Mehata. "WSe_2 quantum dots: A fluorescent probe for ...	<1%
3	Internet	www.mdpi.com	<1%
4	Student papers	Glyndwr University on 2026-07-27	<1%
5	Internet	www.dbd.puc-rio.br	<1%
6	Student papers	Moodle2025 on 2026-08-03	<1%
7	Publication	Zihao Dong, Jie Qi, Lin Yue, Han Zhou, Lu Chen, Jiangjiang Gu, Ying He, Honghong ...	<1%
8	Student papers	Glasgow Caledonian University on 2023-12-19	<1%
9	Student papers	Jamia Milia Islamia University on 2024-06-13	<1%
10	Publication	Song, Yujin. "Recycling of Waste Blood Into Functional Carbon Nanoparticles", Na...	<1%

11 Internet

ijpsr.com <1%

12 Internet

www.rsm.global <1%

13 Internet

ejournals.itda.ac.id <1%

14 Internet

www.researchsquare.com <1%

15 Student papers

College of Public Health on 2026-03-16 <1%

16 Student papers

Macquarie University on 2024-09-16 <1%

17 Publication

Isha, Aneesha, Mohan Singh Mehata. "Synthesis of Graphene Quantum Dots (GQ... <1%

18 Internet

cajmns.centralasianstudies.org <1%

19 Student papers

Anglo-Chinese School (Independent) on 2026-05-27 <1%

20 Publication

Liu, Ming-Wei. "Dynamic Weakening and Trained Memory in Avalanche Dynamics... <1%

21 Student papers

Syiah Kuala University on 2026-08-01 <1%

22 Internet

ejurnal.undana.ac.id <1%

CHAPTER -1

INTRODUCTION

1.1 QUANTUM DOT

As in 2026, with rapid economic and industrial development and population growth, we need critical measures towards sustainability, and a shift toward eco-friendly methods is no longer an alternative but of mainstream importance. The unsustainable use of natural deposits has led to their exhaustion and caused significant ecological damage. When explored sustainably, these resources are replenished constantly, thus increasing bio-capacity and reducing ecological footprint [1]. Chemical contamination has become a major issue, contributing to the rise in toxicity in terrestrial as well as aquatic ecosystems. Addressing global degradation involves remodelling of industrial processes into environmentally friendly and green systems. [2].

The take-make-waste cycle expounds a conventional linear economic model, which is highly unsustainable. As per the 2017 report, we have harvested almost three and a half times more natural resources from Earth's surface than in 1970, and it is likely to double by 2060. The circularity gap report reveals a decline in global circularity from 9.1% in 2017 to 6.9% in 2024 [3]. Hence, if not monitored wisely, global waste production will rise by 70% above today's level by the end of 2050. Subsequently, this widens the gap between extraction and reclamation and eventually exhausts all of Earth's natural resources. [4]

Migration towards the circular economy becomes not just a theoretical preference but a strategic necessity. This requires engineering products that are for reusability, recyclability, and industrial symbiosis. The circular economy provides the infrastructure for value retention by embedding reuse and reparability into the product lifecycle. According to the World Resources Institute, the circular economy can reduce the use of Primary resources by 32 per cent within 15 years and by 53 per cent by 2050. This comes to the fore as a model for material reuse organizations [5].

Green chemistry is an emerging trend that operates at the molecular level to achieve sustainability. This discipline focuses on harnessing chemical innovation to meet ecological and economic goals simultaneously. The Twelve Principles of Green Chemistry provide an integrated framework and foundation for sustainable molecular design [6]. This approach aims to prevent the release of harmful chemicals into the environment, designing less hazardous chemical synthesis that is cost-effective and promotes alternative technologies that have minimal impact on human health and ecosystems [7].

Nanotechnology and advanced functional materials emerged as converging technologies for the successful realization of Society 5.0. These materials directly address the triple environmental crisis by optimizing resource recovery, reducing carbon footprints, and ensuring potable water security. Simultaneously, the integration of nanostructured biomaterials into the healthcare paradigm through personalized, proactive, real-time physiological monitoring [8].

In the realm of nanotechnology, precise optical manipulation provides quantum dots (QDs) with a distinct competitive edge. QDs have a small size but are larger than nanoparticles. They are artificial atoms having a diameter typically between 2 and 10 nm. The most attractive property of QDs is the tunability of emitting light, just by changing particle size. The Manufacturing and Utilization of QDs are increasing, and subsequently their concentration in the environment. Lately, QDs were developed from lead, cadmium and mercury, which raise concerns due to the inherent toxicity of these heavy metals. To attenuate risks associated with environmental contamination, the development of non-hazardous and environmentally friendly (eco-friendly) QDs has become crucial [9].

Carbon is prevalent in nature, occurring in form of diamond (sp^3), graphite (sp^2), fullerenes (sp^2), carbine (sp), amorphous carbon (mixed sp^2 and sp^3), etc. Lately, nanomaterial's based on carbon nanotubes [10], fullerene derivatives , graphene derivatives [11], and CQDs have been areas of interest. However, carbon nanotubes, fullerene derivatives, and graphene derivatives possess poor water solubility, making it difficult to have stability in the emission of fluorescence in visible light. [12]. Carbon quantum dots (CQDs, C-dots or CDs) are popular among QDs due to their high photoluminescence, light resistance, superior biocompatibility, chemical stability, sensitivity via fluorescence quenching and water stability. These are zero-dimensional (0D) nanomaterials having a size less than 10 nm [13]. They show specific electronic transitions, transition for aromatic C=C bond and transition for surface functional groups like C=O or C-N.

Preparation of CQDs is experiencing explosive development, leading to expansion in both bottom-up and top-down synthetic methods. These methods are classified on the basis of the starting point of the material. QDs synthesised by breaking down large, solid carbon into nanosized particles are top-down syntheses; also, the synthesis of QDs by assembling small molecules into a nanocrystal is a bottom-up syntheses. Starting point material for the top-down method is bulk materials like graphite, coal, carbon nanotubes, carbon fibres, or coal. Chemical methods like laser ablation, arc discharge, and electrochemical oxidation are used, where an external force is used to break down the bulk structure. In the bottom-up method, precursors (natural extract, urea, ionic liquids, citric acid, glucose, etc.) are used to synthesis. However, sometimes it requires the use of toxic chemicals for synthesis, which is still a threat. Hydrothermal synthesis can be employed to overcome such barriers due to its non-toxic and cheap practices [14].

With global carbon footprints getting bigger, biomass has become a significant player in making carbon quantum dots (CQDs). This renewable resource, which includes things like plant materials, household trash, and animal waste, can turn would-be garbage into valuable materials. Parts of this biomass, particularly the lignin found in plant fibers, are packed with structures that include carbon and something called heteroatoms – making them perfect for creating these useful quantum dots. But there's a catch. Each type of biomass has its unique chemical makeup, complicating the exact preparation of CQDs. Because of this, it's challenging to come up with straightforward methods to make these materials efficiently, leading to not-so-impressive mass and quantum yields. So while we've got great starting materials, turning them into CQDs remains tricky.

Bio-Mass-derived QDs are gaining prominence over conventional QDs, also for their high biocompatibility and minimal ecological footprint. These QDs exhibit superior photo stability, Tuneable Optical Properties, and high water Solubility. The desperation to shift toward QDs by green methods is growing as it reduces environmental degradation and health issues by reducing dependency on heavy toxic elements. Green synthesis opens the way from waste to wealth by using agricultural waste as a precursor, like waste chicken bones, fruit peels, lignin, etc. This helps diminish environmental as well as health issues (destroy habitats, odour and fire hazards, respiratory problems, cancer in nearby communities) caused by landfilling waste. Its current use is, however, inefficient as most of the agricultural by-products (crop straws) are burned or landfilled, which leads to atmospheric pollution. As abundant and renewable resources are used, it leads to a cost-effective alternative to chemically synthesised QDs.

A sustainable one-pot hydrothermal method was employed for the synthesis; this approach obeys an eco-friendly route over traditional chemical vapour deposition and thus avoids the need for secondary surface passivation agents or hazardous organic solvents. By reducing the need for multiple synthesis steps, this one-pot technique maximises the integration of raw materials into the final product, resulting in significantly less waste production. The ions of the heavy metals bind to the functional groups on the QD's surface, which results in the sensing mechanism. The enhanced sensitivity is achieved by doping a nitrogen heteroatom, which introduces chemically active sites, resulting in high affinity toward heavy metals. This study focuses on the structural engineering of N-CQDs to evaluate their readiness as optical probes. To synthesize CQDs, amla is selected as a precursor for the carbon source. Further, extensive experimental investigations were conducted to understand the morphology and size of the synthesized CQDs. While biomass-derived QDs are employed for fluorescence bio-imaging and anti-counterfeiting ink applications due to their superior biocompatibility and high quantum yield, this work pivots toward environmental metrology [15]

1.2 LITERATURE REVIEW

1.2.1 SYNTHESIS METHODS OF QUANTUM DOTS

There are basically two ways of making quantum dots.

Top-down techniques are used to break down large quantities of materials into nano sized particles using laser ablation, arc discharge, and electrochemical oxidation. These methods provide limited size and surface control.

Bottom-up techniques involve a reaction such as a hydrothermal, solvothermal reaction, microwave, or thermal decomposition, using small organic molecules, providing a certain degree of control over their fabrication, which can lead to biomass-based carbon quantum dots.

1.2.2 GREEN SYNTHESIS

The green synthesis approach has emerged as a sustainable alternative to conventional chemical methods, emphasizes the utilization of naturally derived, non-toxic precursors and eco-friendly solvents, coupled with energy-efficient reaction conditions, thereby minimizing ecological footprint while achieving efficient nanomaterial production.

1.2.3 PRECURSORS

While concerning the precursors in synthesis, it refers to the initial compound that will be involved in synthesizing the end product via a series of reactions. In this case, the definition of precursors becomes the main component in preparing the nanoparticles such as Carbon Quantum Dots (CQDs). This can be achieved through the use of green precursors as opposed to conventional precursors. By doing so, it is possible to come up with technologies that are environmentally friendly. Instead of using toxic components such as the petroleum derivatives, the researcher utilizes green components such as agricultural by-products and plant extracts.

1.2.4 COMMON GREEN METHODS

As far as the synthesis of Carbon Quantum Dots (CQDs) is concerned, the green technology is involved which refers to the so-called "**bottom-up**" approach. This means that the synthesis will be performed by polymerizing and carbonizing the biomass and organic compounds precursors using moderate conditions. Among other technologies available for the synthesis of Carbon Quantum Dots, the most often used one is **hydrothermal/solvothermal** technology. This means that the materials precursors are dissolved in a water/ ethanol solution and heated up to 150-200°C in an autoclave to produce Carbon Quantum Dots. Another popular technology for synthesis is **microwave technology** which presupposes exposing the reactant mixture to microwave radiation in order to synthesize Carbon Quantum Dots in just several minutes. Also, there is **ultrasound technology** used in the synthesis of Carbon Quantum Dots which involves applying ultrasonic waves for heating up the reaction media to obtain Carbon Quantum Dots. This technology allows synthesizing Carbon Quantum Dots at room temperature.

1.2.5 CARBON

The versatility of structure in carbon atoms is due to its electronic arrangement, which is ($1s^2 2s^2 2p^2$). Carbon atoms have four valence electrons that can bond covalently in order to gain stability. The ability to create four bonds with four other elements gives rise to tetravalency. Unlike other atoms that bond using atomic orbitals, carbon atoms are involved in orbital hybridization, a phenomenon in which outer atomic orbitals such as 2s and 2p orbitals come together to produce completely new orbitals designed for molecular bonding. Three types of orbital hybridization can be performed by carbon atoms, namely, sp^3, sp^2 and sp, giving rise to different geometric structures such as tetrahedron (sp^3) , trigonally planar (sp^2), and linear (sp). Allotropy arises out of this diversity in the structural geometry and causes an element to appear in totally different physical forms based on how it is structured; examples include diamond (sp^3) and graphite (sp^2). Carbon, when found in disordered forms in CQDs' cores, exists in a complex hybrid network made up of sp^2 and sp^3 domains. [16]

9
1.2.6 CARBON QUANTUM DOT

Carbon quantum dots (CQDs) are recently discovered 0D carbon-based nanomaterials characterized by quasi-spherical shapes with the size of less than 10 nm. CQDs were unexpectedly obtained in 2004 during the isolation of carbon nanotubes. CQDs are comprised of the core-shell structure, where a core of crystalline or amorphous carbon (sp^2/sp^3) is surrounded by a shell comprising hydrophilic functional groups such as hydroxyl, carboxyl, and amino groups. The primary factor that makes CQDs special and far superior to traditional QDs (for instance, CdSe) based on metals is the presence of optical properties including luminescence and biocompatibility, in addition to high stability and low toxicity, as well as inexpensive synthesis from naturally available materials. For these reasons, CQDs have wide application potential in such fields as biological imaging, drug delivery, chemosensing, solar energy generation, and waste management [17].

CHAPTER -2

EXPERIMENTAL

2.1 MATERIAL AND REAGENT

The synthesis was conducted using commercially available analytical-grade chemicals without any prior purification. Fresh Indian *Phyllanthus emblica* (gooseberries) were procured from the local markets of Delhi, India. Aqueous ammonia (NH_4OH), along with deionized water (DI) of ultrapure grade used in all experiments.

2.2 SYNTHESIS METHODS

2.2.1 Hydrothermal synthesis of Carbon Quantum Dot

250 gm of fruit was thoroughly washed, cut into small pieces, and mechanically crushed to form a uniform pulp. The pulp was passed through a fine metallic stainer, and the collected extract was further purified using Whatman filter paper. For precursor preparation, 27 mL of the fruit extract was diluted in 34 mL of DI water under constant magnetic stirring. To this solution, 2 mL of Aqueous ammonia was added dropwise at a constant interval of time. A visible color transition from light green to brown was observed during the reaction. The resulting mixture was subjected to hydrothermal conditions at 200 °C for 12 h. After natural cooling for 4 h, the product was centrifuged for 30 min at 7000 rpm and filtered through Whatman 40 filter paper. The final dark brown colloidal solution containing QDs was collected and preserved for subsequent analysis.

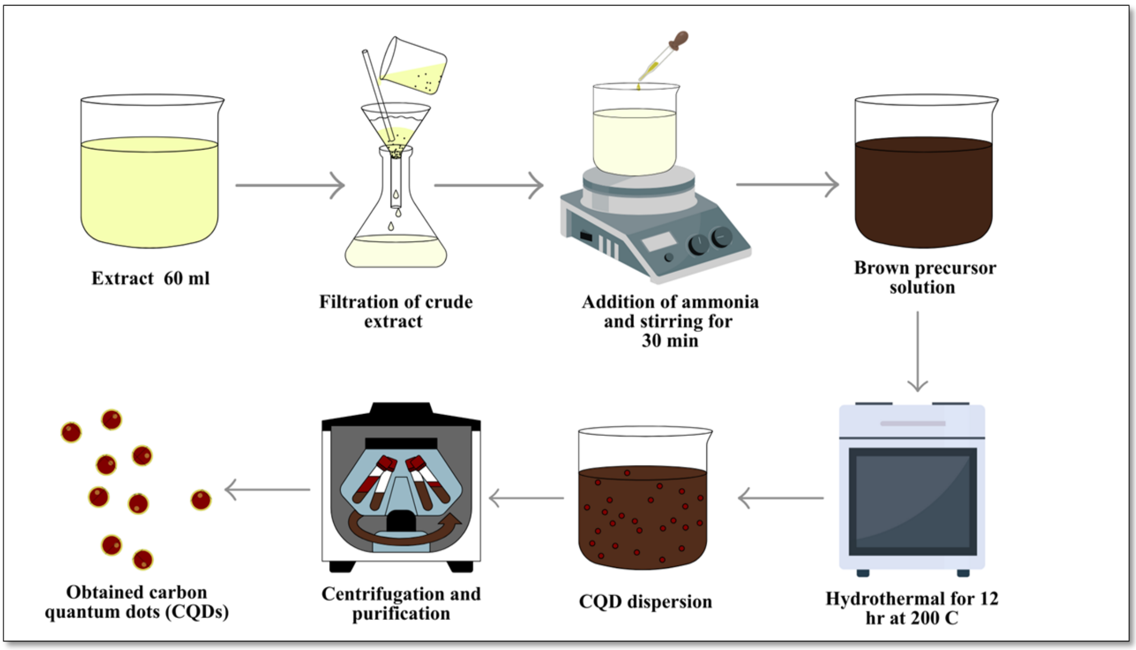

Diagram. 1. Schematic diagram of synthesis process

CHAPTER -3

CHARACTERIZATION AND RESULTS

3.1 Characterization Techniques

To verify that the synthesis is successful and also to analyze the properties of obtained QDs, characterisation tools are used. Dual beam UV-Vis spectroscopy (Model: UV-1900I,SHIMADZU) is use to study the UV-Vis spectroscopy. Analysis of PL and PL-excitation is done using the Fluorolog-3 spectrofluorometer (Horiba Jobin Yvon), set up with a PMT, 450W Xenon, and flash lamps. XRD patterns are obtained by using Bruker D8 advance having Cu(Kα) radiation source with an accelerating voltage of 40KV and a current of 20 mA. High-resolution images of CQDs are captured using TEM technique, operates at an accelerating voltage of 200 KV. FTIR spectra is obtained using Model No.- Nicolet iS50 FTIR spectrometer.

3.2 Results and discussion

3.2.1 X- RAY DIFFRACTION (XRD)

To analyze the structure of Amla extracted CQDs, the XRD pattern of the synthesized CQDs has been studied as illustrated in Fig.1. The diffractograms of the synthesized CQDs exhibited numerous diffraction peaks at Bragg angles 2θ =26.44º, 43.92º, 54.62º, and 77.52º. A prominent diffraction peak was observed at 26.44°, corresponding to the (002) plane [14], [18], [19] and peaks at 43.92° and 54.62°, which were indexed to the (100) and (102) planes of the carbon phase, respectively. Here, the 77.52° peak is not identified; this is likely caused by imperfections or impurities in the material [14]. The simultaneous presence of graphitic

(002) and (102) reflections confirms the coexistence of sp^2 graphitic carbon [20] and the broadening at the base of the peak shows the presence of an amorphous surface layer [21].[22]. The average dimensions of the synthesized QDs were calculated using the Debye-Scherrer equation.

$$D = \frac{k\lambda}{\beta cos\theta} \qquad (1)$$

2

where k is the geometric factor (0.94), λ is the wavelength of the X-ray associated with the copper radiation source, θ is the angle of the diffraction peak, and β is the FWHM of the observed peak. The average calculated Crystallite Size (well-ordered core) of the synthesized CQDs using Eq. (1) were approximately 2.40 nm. [23] [19]. Calculating for d-spacing ($n\lambda = 2d \sin\theta$), it came out to be 3.368 A° which is close to natural graphite (3.354 A°) show high crystalline quality and interlayer spacing belong to (002) plane [24].

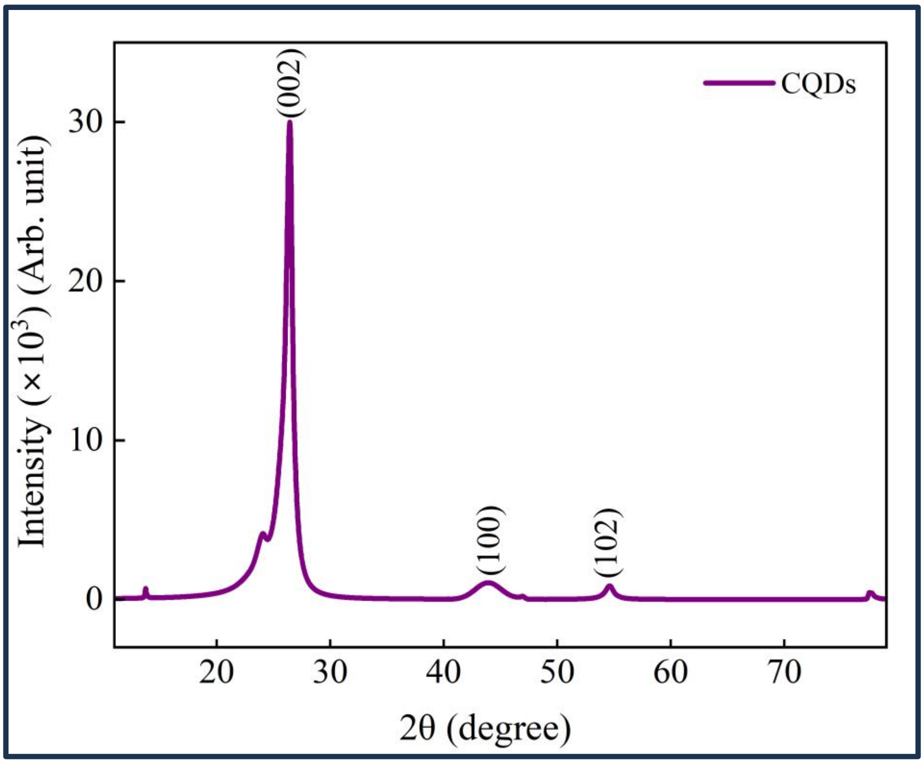

Fig .1. XRD pattern of synthesized CQDs deposited on the glass substrate thin film.

11

3.2.2 HIGH-RESOLUTION TRANSMISSION ELECTRON MICROSCOPY (HR-TEM)

The morphology and size distribution of the synthesized CQDs were investigated using HR-TEM, as shown in Fig.2. [25]. The synthesized CQDs are distributed between 2.0 and 4.5 nm, and with an average particle size of 2.93 ± 0.03 nm. The selected area electron diffraction (SAED) images also show the slightly blurry rings rather than single spots, as CQDs are tiny and randomly oriented, confirming a polycrystalline sample [14]. The pattern displays three broad diffuse concentric rings, which can be loosely indexed to the (002), (100) and (102) planes of carbon. Further, calculating d-spacing from SAED image shows in-plane lattice spacing of 0.26 nm belongs to (100) plane [26].

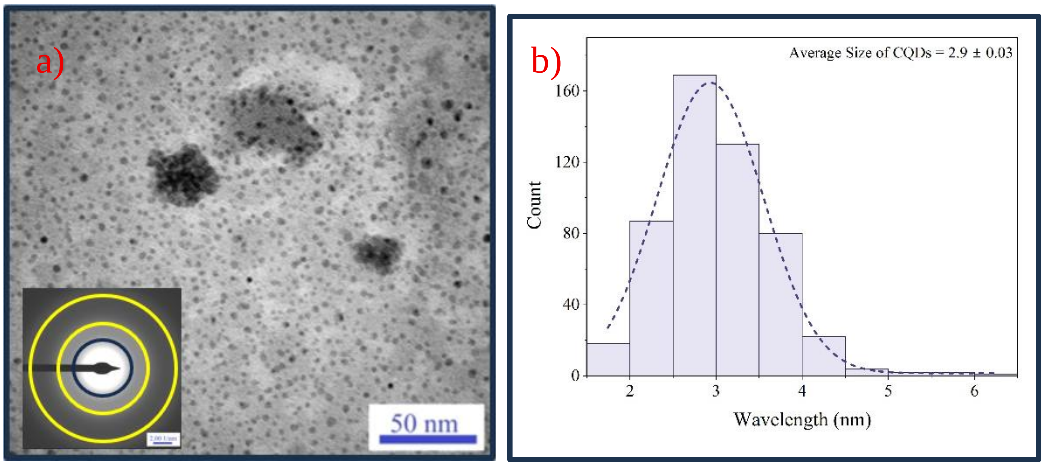

Fig. 2. HR-TEM micrographs of synthesized CQDs (a) with corresponding particle size distribution (b). Inset of (a) displays the SAED pattern of synthesized CQDs.

5

3.2.3 FOURIRE-TRANSFORM INFRARED SPECTROSCOPY (FTIR)

Fig. 3 shows the FT-IR spectrum of the synthesized CQDs. The FTIR spectrum displays several peaks related to the surface bonds of the synthesized CQDs. FTIR analysis revealed an absorption band at approximately 3390 cm^{-1}, attributed to O-H and N-H stretching vibrations, which confirmed the presence of amino and hydroxyl groups. The peak at approximately 2969 cm^{-1} corresponds to the C-H stretching. A peak at approximately 1720 cm^{-1} corresponds to C=O stretching of carboxyl groups. The peak at 1631 cm^{-1} is attributed to C=C/C=N stretching vibrations, Surface groups are indicated by C-O/C-N stretching at 1140 cm^{-1}; the presence of C-N bonds provides direct evidence of the successful incorporation of nitrogen into the carbon lattice [27], [28]. The presence of these surface groups is critical because they provide surface traps for applications. These oxygen- and nitrogen-rich functional groups create surface defect states (surface traps) that facilitate the radiative recombination of excitons, which is the primary mechanism for the high photoluminescence quantum yield of these QDs. The abundance of hydrophilic groups ensures excellent dispersibility in aqueous media and provides long-term colloidal stability without the need for additional surfactants in the synthesis

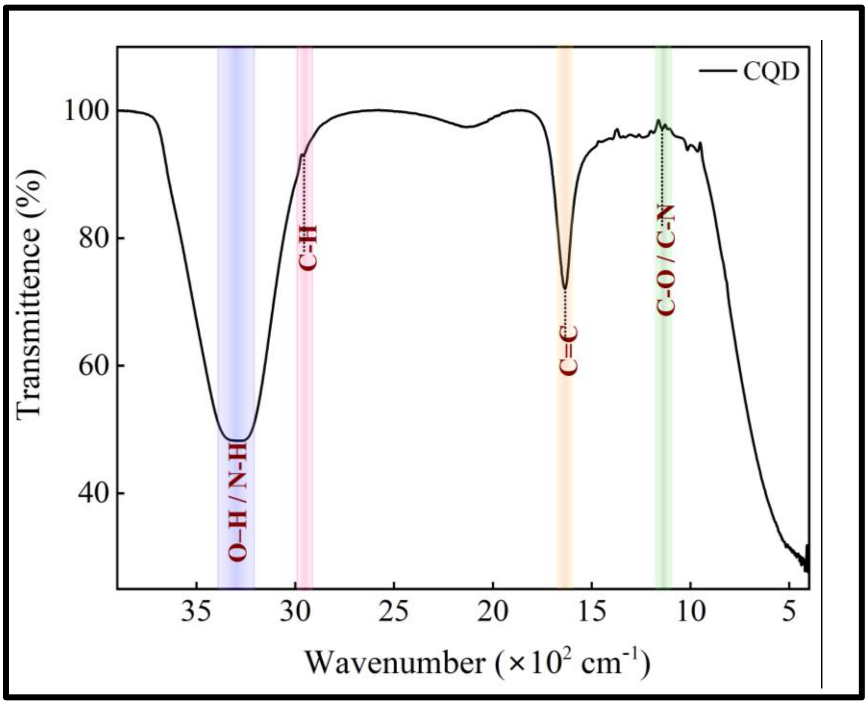

Fig. 3. FTIR spectrum of CQDs dispersed in aqueous medium.

3.2.4 ULTRAVIOLET –VISIBLE (UV-Vis)

The photophysical performance and properties of the CQDs were analysed using UV-Vis spectroscopy. Biomass-derived CQDs are usually seen to have obvious absorption in the ultraviolet region. Fig. 4. shows the absorption spectrum of the synthesized CQDs, which exhibits distinct peaks at 252 nm (4.92 eV), 295nm (4.20 eV) and 373 nm (3.32 eV). The observed peak at 252 nm corresponds to a π–π* transition, which justifies the C=C bond within the aromatic sp^2 domains of the synthesized CQDs [29]. The second peak at 295 nm corresponds to the n–π* transitions that confirm the presence of oxygenated functional groups, like C=O and C–N/C=N bonds, hence n-doping, as depicted in the FTIR spectrum [30]. A weak shoulder is also observed around 373 nm, a common characteristic feature reported for nitrogen- and oxygen-rich CQDs synthesized via hydrothermal carbonization[29].The literature suggests that nitrogen-doping can significantly enhance their optical properties and sensing performance by changing their electronic characteristics, defect degree, and band structure.[25] , [31].

The 2^{nd} derivative was calculated to resolve overlapping absorption bands that are not clearly distinguishable in the conventional uv-vis spectrum. The 2^{nd} derivative spectrum revealed three negative minima curves, which clearly identified three centers at 252, 295, and 373 nm. Beyond 400 nm, the 2^{nd} derivative spectrum becomes flat, confirming the absence of any absorption in the visible region.

3.2.5 PHOTOLUMINESCENCE (PL)

PL spectroscopy was used to investigate the fluorescence property of the synthesized CQDs. The composition of biomass-derived CQDs varies by source, directly affecting their fluorescence properties. The CQDs synthesized from biomass are often reported to have low photoluminescence quantum yield and poor optical properties. The synthesized sample appears yellowish under visible light and emits blue fluorescence when viewed under a UV lamp. Fig.5. shows the combined absorption spectrum, PL spectrum with an excitation of 340 nm and PL-excitation spectrum (PLE) at 420 nm. The PL emission of the sample clearly depicts the excitation-dependent PL, which is advantageous for a variety of applications. [31]. The figure depicting the PL spectra for excitation wavelengths from 290 to 450 nm shows an increase in PL intensity from 290 to 340 nm, followed by a gradual decrease. The optimal excitation wavelength of 340 nm is reported to give maximum emission. A red shift of 88 nm is shown by the normalized PL spectra in Fig, The nitrogen doping alters the surface state of CQDs by generating new energy levels which reduces the energy gap and hence results in a significant red shift in the fluorescence emission wavelength. [32] PLE was recorded by observing the emission at various wavelengths. A dominant peak was observed at 420 nm emission wavelength. The presence of well-defined dominant peak in the PLE spectrum confirms that the photoluminescence originates from a specific electronic transition intrinsic to the N-CQD structure.

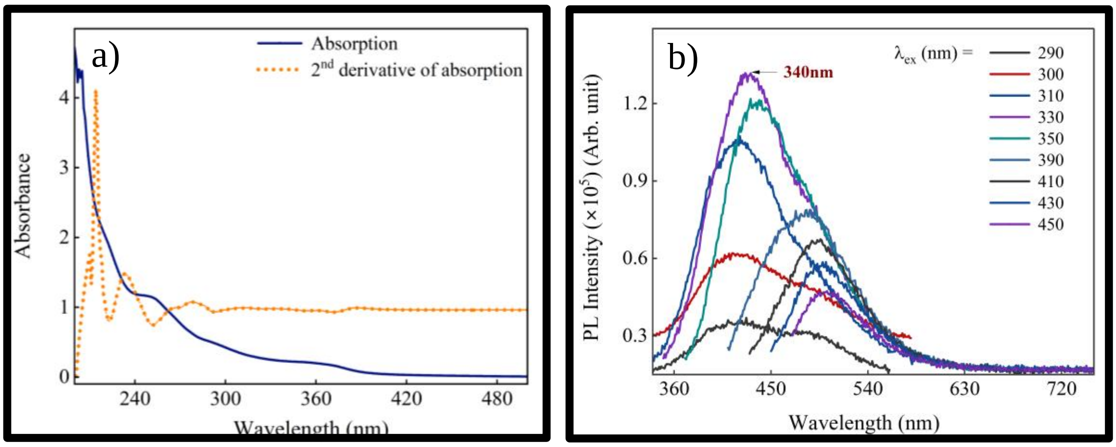

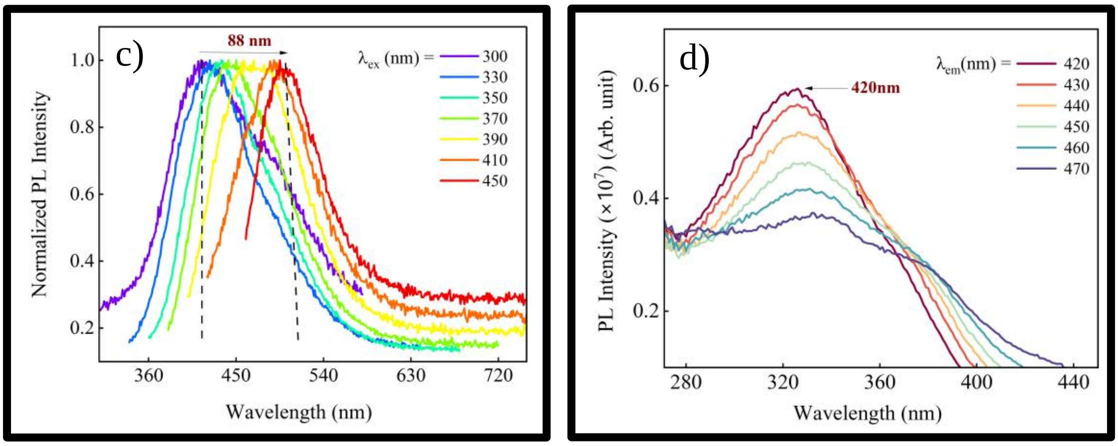

Fig. 4. a) Absorption spectrum of synthesized CQDs overlapped with its 2nd order derivative, b) PL spectra of CQDs recorded at various excitation wavelengths, c) Normalized PL spectra to highlight PL shift and profile consistency, d) PL excitation spectra of CQDs

CHAPTER -4

4.1 CONCLUSION

Based on the results of the experiment, it should be noted that the process of obtaining nitrogen-doped carbon quantum dots (N-CQDs) via hydrothermal synthesis from *Phyllanthus emblica* (gooseberries) yielded nano crystals 2.93 ± 0.03 nm in size. From the characterization results obtained through XRD and HR-TEM methods, it can be said that the composite material consists of a crystal structure of type $sp^2$and the d-spacing equal to 3.368Å, similar to that in graphite. Based on the composition analysis of synthesized nanoparticles, it was shown that nitrogen was incorporated, along with oxygen-containing functional groups, namely, hydroxyl, amino, and carboxyl groups. The characterization of synthesized N-CQDs made it possible to identify the specificities of the absorption spectrum, containing two peaks of 252 and 295 nm, corresponding to $\pi \rightarrow \pi^*$ and $n \rightarrow \pi^*$ transitions, correspondingly. Attention should be paid to the feature of excitation-dependent photoluminescence of N-CQDs, causing blue luminescence at 420 nm with excitation at 340 nm.

4.2 FUTURE SCOPES

As regards the N-CQDs that have been discussed in this work, their future perspectives can utilize their enhanced nitrogen sensing capabilities and tunable optical properties, which can be used in creating new types of sensors and optoelectronics. In addition, their enhanced features of hydrophilicity and colloidal stability, obtained through introducing oxygen and nitrogen-containing functional groups into the structure, can be applied in biological spheres, such as imaging and molecule docking. As regards the social aspect, the green hydrothermal synthesis provides an ecologically safer option than toxic semiconductors.

REFRENCES

[1] X. Zheng *et al.*, "Global environmental impacts of nanomaterials: A systematic review," *Frontiers in Environmental Science*, vol. 12, p. 1368125, 2024. doi: 10.3389/fenvs.2024.1368125.

[2] Y. Liu *et al.*, "Advanced synthesis of carbon dots for biomedical engineering applications," *Carbon Research*, vol. 3, no. 1, 2024. doi: 10.1007/s44274-024-00033-5.

[3] M. Alizadeh *et al.*, "Managing technical change and green innovation pathways," *Economics of Innovation and New Technology*, vol. 35, no. 2, pp. 112–128, 2026. doi: 10.1080/13662716.2026.2626376.

[4] J. R. Smith *et al.*, "Evaluating sustainable development indicators in manufacturing sectors," *Sustainability*, vol. 14, no. 3, p. 1757, 2022. doi: 10.3390/su14031757.

[5] T. Wang *et al.*, "Deep learning models for surface defect detection in industrial automation," *Applied Sciences*, vol. 12, no. 3, p. 1521, 2022. doi: 10.3390/app12031521.

[6] P. John *et al.*, "Synthesis and characterization of functionalized graphene oxides," *Journal of Materials Chemistry*, vol. 20, no. 11, pp. 2145–2152, 2010. doi: 10.1039/B918763B.

[7] S. Kumar *et al.*, "Nanotechnology solutions for water purification systems," *Clean Water Technologies*, vol. 2, no. 1, 2025. doi: 10.1007/s44371-025-00152-9.

[8] L. Zhang *et al.*, "Carbon quantum dot-based composites for high-performance supercapacitors," *ACS Nano*, vol. 15, no. 12, pp. 19543–19555, 2021. doi: 10.1021/acsnano.1c10919.

[9] H. Zhao *et al.*, "Fluorescent properties of biomass-derived carbon dots," *Nanoscale Research Letters*, vol. 20, no. 1, 2025. doi: 10.1186/s11671-025-04323-6.

[10] Y. Zhang, L. Wang, and H. Chen, "Green synthesis of carbon quantum dots: A review," *Journal of Nanoparticle Research*, vol. 22, no. 8, p. 234, 2020.

[11] M. Clancy, J. B. O'Connor, and R. Murphy, "Environmental life cycle assessment of

bio-based plastics," *Journal of Cleaner Production*, vol. 182, pp. 312–323, 2018.

[12] K. Tanaka *et al.*, "Stress analysis and mechanical performance of nanomaterial alloys," *Journal of Stress Analysis*, vol. 41, p. 100411, 2024. doi: 10.1016/j.stress.2024.100411.

[13] X. Yang *et al.*, "Preparation of cellulose-derived nanomaterials from agricultural waste," *BioResources*, vol. 19, no. 3, pp. 4512–4527, 2024. doi: 10.15376/biores.19.3.Yang.

[14] G. Singh *et al.*, "High-efficiency perovskite solar cells via molecular passivation," *Scientific Reports*, vol. 13, p. 18942, 2023. doi: 10.1038/s41598-023-46084-1.

[15] J. Yang *et al.*, "Biomass carbon quantum dots: Fabrication, properties, and sensing applications," *Materials Today Chemistry*, vol. 36, p. 101924, 2024.

[16] F. Robert *et al.*, "Advanced manufacturing review for smart composite surfaces," *Manufacturing Review*, vol. 10, p. 11, 2023. doi: 10.1051/mfreview/2023011.

[17] R. M. Peterson *et al.*, "Supramolecular assemblies of carbon-based nanomaterials," *Small Science*, vol. 1, no. 4, p. 2000023, 2021. doi: 10.1002/nano.202000232.

[18] A. Khan *et al.*, "Optical properties of sulfur-doped carbon quantum dots," *Materials Research Express*, vol. 6, no. 8, p. 081450, 2019. doi: 10.1088/2053-1591/ab1450.

[19] H. Zhou *et al.*, "Design of high-precision optical lenses using nanostructured coatings," *Optik*, vol. 301, p. 171725, 2024. doi: 10.1016/j.ijleo.2024.171725.

[20] T. Jenkins *et al.*, "Nanoscale surface modification for biochemical sensors," *Small Science*, vol. 5, no. 2, p. 70090, 2025. doi: 10.1002/nano.70090.

[21] S. Ahmed *et al.*, "Eco-friendly synthesis of silver nanoparticles using plant extracts," *Progress in Biomaterials*, vol. 8, no. 3, pp. 157–166, 2019. doi: 10.1007/s40089-019-0271-9.

[22] M. R. Al-Mulla *et al.*, "Synthesis of biocompatible carbon dots for selective metal ion sensing," *RSC Advances*, vol. 13, no. 34, pp. 23812–23821, 2023. doi: 10.1039/d3ra04018f.

[23] J. Lee *et al.*, "Piezoelectric properties of lead-free ferroelectric thin films," *Ferroelectrics*, vol. 560, no. 1, pp. 88–95, 2020. doi: 10.1080/00150193.2020.1762435.

[24] W. Zhang *et al.*, "Nitrogen-doped carbon dots for cellular imaging and free radical scavenging," *ACS Omega*, vol. 5, no. 31, pp. 19622–19631, 2020. doi: 10.1021/acsomega.0c03290.

[25] R. M. Peterson *et al.*, "Supramolecular assemblies of carbon-based nanomaterials," *Small Science*, vol. 1, no. 4, p. 2000023, 2021. doi: 10.1002/nano.202000232.

[26] C. Wang *et al.*, "Electrochemiluminescence sensors utilizing functionalized quantum dots," *RSC Advances*, vol. 13, no. 12, pp. 8142–8150, 2023. doi: 10.1039/d3ra01646c.

[27] Nature Portfolio, "Scientific Reports collection updates," *Scientific Reports*, 2024. [Online]. Available: http://www.nature.com/scientificreports.

[28] Y. Kim *et al.*, "Mechanical properties of 3D-printed biopolymer scaffolds," *Materials*, vol. 15, no. 2, p. 466, 2022. doi: 10.3390/ma15020466.

[29] D. Evans *et al.*, "Anomalous thermal expansion in framework materials," *Scientific Reports*, vol. 15, p. 3421, 2025. doi: 10.1038/s41598-025-29913-3.

[30] K. J. Choi *et al.*, "Antibacterial activity of green-synthesized zinc oxide nanoparticles," *Scientific Reports*, vol. 12, p. 12451, 2022. doi: 10.1038/s41598-022-16893-x.

[31] K. J. Choi *et al.*, "Antibacterial activity of green-synthesized zinc oxide nanoparticles," *Scientific Reports*, vol. 12, p. 12451, 2022. doi: 10.1038/s41598-022-16893-x.

[32] H. Liang *et al.*, "Ultrafast laser micro-machining of advanced optical crystals," *Light: Advanced Manufacturing*, vol. 4, no. 4, pp. 385–396, 2023.